Discretization of Time-Dependent Quantum Systems: Real-Time Propagation of The Evolution Operator

Joseph W. Jerome*and Eric Polizzi†

Abstract

We discuss time dependent quantum systems on bounded domains. Our work may be viewed as a framework for several models, including linear iterations involved in time dependent density functional theory (TDDFT), the Hartree-Fock model, or other quantum models. A key aspect of the analysis of the algorithms is the use of time-ordered evolution operators, which allow for both a well-posed problem and its approximation. The approximation theorems obtained for the time-ordered evolution operators complement those in the current literature. We discuss the available theory at the outset, and proceed to apply the theory systematically in later sections via approximations and a global existence theorem for a nonlinear system, obtained via a fixed point theorem for the evolution operator. Our work is consistent with first-principle real time propagation of electronic states, aimed at finding the electronic responses of quantum molecular systems and nanostructures. We present two full 3D quantum atomistic simulations using the finite element method for discretizing the real-space, and the FEAST eigenvalue algorithm for solving the evolution operator at each time step. These numerical experiments are representative of the theoretical results.

AMS classification numbers: 35Q41, 81-08, 47D08, 81Q05

Key words: Time dependent quantum systems; TDDFT; time-ordered evolution operators; Hamiltonian; potential functions; Gauss quadrature

.

.

[1]Department of Mathematics, Northwestern University, Evanston, IL 60208

[2]Department of Electrical and Computer Engineering, University of Massachusetts, Amherst, MA 01003

1 Introduction

This article analyzes a general version of time dependent quantum mechanical systems via time ordered evolution operators. Time-ordered evolution operators arise from direct integration of the time-dependent Schrödinger equation. They are most often used to enable real-time propagation of ground-state solutions in response to any arbitrary external perturbations of the quantum system. Important physics can be extracted from the time-domain responses. The development of efficient numerical techniques which aim at achieving both accuracy and performance in time-dependent quantum simulations has become important for a large number of applications spanning the fields of quantum chemistry, solid state physics and spectroscopy. In particular, finding a suitable numerical representation for the time-ordered evolution operator is one of the main focuses of the TDDFT research field [1].
The numerical treatment of time-ordered evolution operators often gives rise to the matrix exponential, commonly treated using approximations such as split-operator techniques [2]. The efficiency of the time-domain propagation techniques described here, however, is further enhanced by reliance on the capabilities of the new FEAST algorithm for solving the eigenvalue problem [3, 4]. By using FEAST, the solution of the eigenvalue problem is reformulated into solving a set of well-defined independent linear systems along a complex energy contour. Obtaining the spectral decomposition of the matrix exponential becomes then a suitable alternative to PDE based techniques such as Crank-Nicolson schemes [5], and can also take advantage of parallelism.
The goals of the paper are as follows.

- To provide a rigorous infrastructure, both on the ground space and the 'smooth' space, for the evolution operator used in topical applications of TDDFT cited in this article (see [6] for an early adaptation of Kato's evolution operator);
- To complement the numerical Gauss quadrature in time introduced in [7] and to provide an exact interface with the use of FEAST; the simulations and theorems of this article are tightly connected;
- To complement the detailed estimates obtained via the Magnus expansion [8, 9] by an alternative approach based on finite element estimation; in particular, the Bramble-Hilbert lemma and the Sobolev representation theorem;
- To introduce the numerical evolution operators; in an approximate sense, this leads to the approximate preservation of significant quantities.
- To obtain, via entirely different methods based on the evolution operator, pertinent existence theorems in the literature [10, 11]; in some cases, more information can be extracted from this approach, including local existence for very general nonlinearities. In particular, our focus on the nonlinear Schrödinger equation with Hartree potential is consistent with

recent studies [12] characterizing this equation as a weak limit of weakly coupled Fermion systems. Our global analytical methods are not applied to obtain uniqueness for nonlinear systems, since this is a well-studied topic.

We summarize now the plan of the paper. In the following section, we outline the mathematical properties developed over the years for Schrödinger operators, as applied to many-particle systems. The section includes a discussion of current understanding and practice. We also introduce the evolution operator and admissible Hamiltonians. In the appendix, we include the basic theory of the evolution operator. This is due to Kato [13, 14] and Dorroh [15], and is detailed in [16]. The appendix includes the verification that the Hartree potential satisfies the required hypotheses for inclusion in the class of admissible Hamiltonians; this leads to invariance of the evolution operator on the smooth space. Section three introduces discretization of the evolution operators, in terms of the traditional rectangular rule, for short time steps, and in terms of 'degree of precision' quadrature rules for longer time steps. Although this resonates with classical theory, the corresponding proofs of the approximation theorems of the following section are not elementary. This is followed in section four by precise statements of the principal theorems and by proofs, which validate the discretizations. In addition, a well-posedness result (global existence in time) is given for the nonlinear Schrödinger equation, involving the Hartree potential coupled to an external potential for a closed system. Numerical simulations and discussions are presented in section five, and future research is outlined in section six. Finally, our analysis is for the bounded domain in Euclidean three space, and excludes the use of Strichartz estimates.

2 Time Dependent Quantum Systems

Two major theories have been developed to analyze many-particle quantum systems. Classical density functional theory (DFT) is derived from the Hohenberg-Kohn theorem in [17]. By transferring inter-electron effects to the exchange-correlation potential, expressed as a functional of the electron density ρ, the theory is capable of representing a many-electron system in terms of non-interacting effective particles. This theory employs pseudo-wave functions but a precise representation for the electron charge density. The aggregate potential is the effective potential V_{eff}. This leads to the Hamiltonian $\hat{H}$ and its associated Kohn-Sham orbitals [18]. Well-posedness of the steady problem has been studied in [19]; applications in [20]. Although DFT is only applicable for obtaining the ground state of quantum systems consistent with charge density, its time-dependent counterpart, TDDFT, has been proposed in [21] to investigate the dynamics of many-body systems and can be potentially used to obtain energies of excited states. Another major theory used in the theoretical chemistry community is the Hartree-Fock model. Here, the emphasis is directed toward the calculation of exact orbitals (for a mathematical discussion, cf. [22]). Aspects

of these two theories are covered in the present framework, as well as other quantum theories.

2.1 Initial value problem for Schrödinger systems

We follow the notation and format of [7]. If we denote by $\hat{H}$ the Hamiltonian operator of the system, then the state $\Psi(t)$ of the closed quantum system obeys the Schrödinger equation,

$$i\hbar\frac{\partial\Psi(t)}{\partial t} = \hat{H}\Psi(t). \tag{1}$$

For mathematical well-posedness, an initial condition,

$$\Psi(0) = \Psi_0, \tag{2}$$

and boundary conditions must be adjoined. In the study [21], it is shown that the initial value problem is well-defined physically; there is an inherent invertible mapping from the time dependent external potential function to the time dependent particle density. This study is now the basis in the physics community for the reliability of physics-based studies involving time dependent density functional theory. An important study using this model is contained in [23]. The model is now characterized as the Runge-Gross model; the potential in the Hamiltonian includes: an external potential, which allows for an ionic component, the Hartree potential, and the exchange-correlation potential. Except for the global existence result for the Hartree potential, the present article is restricted to potentials which are linear in the quantum state, but the theory has the capacity to extend to local (in time) nonlinear versions of the Runge-Gross model. We will assume that the particles are confined to a bounded region $\Omega \subset \mathbf{R}^d$, with $d = 1, 2, 3$, and that homogeneous Dirichlet boundary conditions hold for the evolving quantum state. In particular, the spectrum of the Hamiltonian is discrete in this case. Also, the proofs are unaffected by the interpretation of Ψ as a scalar or vector complex-valued function.

2.2 Specification of the Hamiltonian operator

Consider a linear problem, i. e. , an external potential $V(\mathbf{x}, t)$ which is independent of the system state, particularly the charge density. This assumption is equivalent to studying a non-interacting system. Alternatively, in the case of an interacting system, it describes exactly one iteration of a nonlinear mapping based on potential which includes the exchange correlation potential, the Hartree potential, or contributions from other quantum system models. It is natural therefore to make the following assumption:
Assumption The Hamiltonian,

$$-\frac{\hbar^2}{2m}\nabla^2 + V(\cdot\,, t), \tag{3}$$

has, for each t, an L^2 self-adjoint extension $\hat{H}(t)$.
It follows from a theorem of Stone [24], [25, Ch. 35, Theorem 1] that, for each fixed t_*, $(\pm i/\hbar)\hat{H}(t_*)$ is the infinitesimal generator of a strongly continuous group, $\{\exp[(\pm i/\hbar)\hat{H}(t_*)t]\}$, of unitary operators on L^2.
The earliest results for the self-adjointness of the Hamiltonian with interactions including Coulomb potentials are attributed to Kato [26, 27]. Since later results by Kato and other authors [28] imply that these operators are also stable in the sense we have defined them, it follows that the framework for evolution operators outlined here covers this case. Moreover, any further perturbation of such potentials by potentials depending (non-linearly) on C^1 class functions of the quantum state, with bounded derivatives, is also admissible. This is a classical commutator result, initially investigated in [29]. The framework here is thus quite general. However, the choice of Y of Theorem A.1 of the Appendix, is strongly dependent on the structure of the effective potential.

2.3 The Hartree potential and admissible external potentials

In this section, all statements pertain to Euclidean space $\mathbf{R}^3$. In order to motivate the format of the Hamiltonian operators for the linear problem, we first consider the initial value problem for the *nonlinear* Schrödinger equation,

$$i\hbar\frac{\partial\Psi(t)}{\partial t} = \hat{H}\Psi(t), \tag{4}$$

where

$$\hat{H}\Psi = -\frac{\hbar^2}{2m}\nabla^2\Psi + V_{\rm ex}\Psi + (W * |\Psi|^2)\Psi.$$

Here, $W(\mathbf{x}) = 1/|\mathbf{x}|$, and the convolution,

$$(W * |\Psi|^2)(\mathbf{x}, t) = \int_\Omega W(\mathbf{x} - \mathbf{y})|\Psi(\mathbf{y}, t)|^2 \, dy_1 dy_2 dy_3,$$

represents the Hartree potential, where we have written $|\Psi|^2$ for the charge density ρ, and $V_{\rm ex} = V_{\rm ex}(\mathbf{x}, t)$ for the external potential. When spin is accounted for, ρ includes an additional factor of two. In the appendix, we are able to show that, for a choice of Hartree potential defined by a charge density of minimal regularity, the Hamiltonian family may be used to construct the evolution operators $\{\hat{U}(t, s)\}$.

3 Discretization Schemes

We begin by introducing a widely used notation in the mathematical physics community (e. g. , see [23]) for the evolution operators $\{\hat{U}(t, s)\}$, which can be useful if the argument (t, s) is not essential, and emphasis is to be placed upon the family of semigroup generators and the semigroups used in the construction

of the evolution operators. Formally, then, the time-ordered evolution operator for (1) takes the form [23]:

$$\hat{U}(t,0) = \mathcal{T} \exp\left\{ -\frac{i}{\hbar} \int_0^t d\tau \hat{H}(\tau) \right\}, \tag{5}$$

and the final solution at time T is then given by:

$$\Psi(T) = \hat{U}(T,0)\Psi_0. \tag{6}$$

This is equivalent to the formula (37) with $F = 0$. Notice that $\hat{U}$ is used here for the quantum mechanical interpretation of evolution operators.
In addition to the final solution $\Psi(T)$, the evolution of the system along $[0, T]$ can be described by intermediate solutions. From the properties of the time-ordered evolution operator (property **II** of Theorem A.1 of the Appendix), one can indeed apply the following decomposition:

$$\hat{U}(T,0) = \hat{U}(t_n, t_{n-1}) \dots \hat{U}(t_2, t_1)\hat{U}(t_1, t_0), \tag{7}$$

where we consider $n-1$ intermediate times with $t_0 = 0$ and $t_n = T$, and where the solution $\Psi(t)$ can be obtained at time t_j, $j = 1 \dots n$. Let us assume a constant time step Δ; the corresponding time-ordered evolution operator is designated

$$\hat{U}(t+\Delta, t) = \mathcal{T} \exp\left\{ -\frac{i}{\hbar} \int_t^{t+\Delta} d\tau \hat{H}(\tau) \right\}. \tag{8}$$

Let us then outline two possibilities: (i) Δ is very small in comparison to the variation of the potential $V(\cdot\,, t)$; and (ii) Δ is much larger.

3.1 Small time-step intervals: the rectangular rule

If Δ is chosen very small such that $\hat{H}(\tau)$ can be considered constant within the time interval $[t, t+\Delta]$, it follows that the argument of the exponential in (8) needs to be evaluated only at time t:

$$\hat{U}_\Delta(t+\Delta, t) \mapsto \exp\left\{ -\frac{i}{\hbar} \Delta \hat{H}(t) \right\}, \tag{9}$$

which is then equivalent to solving a time independent problem along Δ. Note that this is equivalent to Definition 4.1, formulated in section 4.1. Additionally, we note that the time-ordered exponential can be replaced by the exponential (semigroup) operator in this case, which is the essence of the rectangular integration rule. Schematically, we write for the semigroup product:

$$\mathcal{T}\left\{ \prod_j S(t_j) \right\} = S(t_N) \dots S(t_2) S(t_1). \tag{10}$$

In section 4.1, we show how the rectangular rule globally defines a family of approximate evolution operators, shown (rigorously) to converge to the time-ordered family. In this case, the approximation operators must be defined so that they also possess the time-ordered property. We have then the following on $[0, T]$:

$$\lim_{\Delta \to 0} \hat{U}_\Delta = \hat{U}. \tag{11}$$

The approximation order is shown to be $o(\Delta)$ in Theorem 4.1.

3.2 Long time-step intervals

In simulations, the use of very small time-step intervals has a sound physical interpretation as it corresponds to a step by step propagation of the solution over time. The major drawback of this approach, however, is that it involves a very large number of time steps from initial to final simulation times. In contrast, much larger time intervals could become advantageous in simulations since the electron density (or other integrated physical quantities) is likely to exhibit much weaker variations as compared to the variations of the individual wave functions. In addition, at certain frequency, e.g. THz, long-time domain response is needed, and accurate calculations using large time steps could be used to speed-up the simulation times. Let us now consider the case of a much longer time interval of length Δ, which may correspond, for instance, to a given period of a time-dependent perturbation potential $V(\cdot, t) = V_0(\cdot)\sin(2\pi t/\Delta)$. A direct numerical integration of the integral component in the time-ordered evolution operator (8), leads to

$$\hat{U}_\delta(t + \Delta, t) = \mathcal{T} \exp\left\{ -\frac{i}{\hbar} \xi \sum_{j=1}^{p} \omega_j \hat{H}(t_j) \right\}, \tag{12}$$

where ω_j and ξ are integration weights, and p is the number of quadrature points. The subscript δ suggests the local construction of the evolution operators within the larger subinterval.

Remark 3.1. *In the case of a rectangular quadrature rule, one notes that* $\omega_j = 1$, $\xi = \delta$, $t_j = t + j * \delta$ *and* $\delta \equiv \Delta/(p+1)$. *Here,* $j = 0, \ldots, p+1$. *Therefore, it follows from (11):*

$$\lim_{p \to \infty} \hat{U}_\delta = \hat{U}.$$

In particular, if the number of rectangle quadrature points p *increases significantly, the problem is then equivalent to solving (9) multiple times since*

$$\hat{U}_\delta(t + \Delta, t) = \prod_{j=0}^{p} \hat{U}_\delta(t_j + \delta, t_j). \tag{13}$$

Clearly, higher-order quadrature schemes such as Gaussian quadrature can use far fewer points p than a low-order quadrature rule such as the rectangular rule,

to yield a high order approximation of the integral of a function. A p-point Gaussian quadrature rule is a numerical integration constructed to yield an exact result for polynomials of degree $2p-1$ by a suitable choice of the points t_i and Gauss-Legendre weights ω_j [30, Sec. 5.5]. We associate the quadrature points t_j at the Gauss node x_j using $t_j = \frac{\Delta}{2}x_j + \frac{2t_0+\Delta}{2}$; also we note $\xi = \Delta/2$. Thus, the following is a reasonable conjecture:

$$\forall \epsilon, \quad \exists p_0 \text{ such that } \forall p \geq p_0, \quad \|\hat{U}_\delta - \hat{U}\| \leq \epsilon.$$

Here, δ represents an average spacing between quadrature nodes: $\delta \simeq \Delta/(p+1)$. In section 4.2, we show that this estimate is rigorously correct for the weighted sum of the Hamiltonians (cf. Theorem 4.2).

3.3 Evaluation of the approximate evolution operator

In order to evaluate the time-ordered evolution operator, it is necessary to decompose the exponential in (12) into a product of exponential operators taken at different time steps:

$$\hat{U}_\delta(t+\Delta,t) = \mathcal{T}\left\{\prod_{j=1}^{p} \exp\left\{-\frac{i}{\hbar}\xi\omega_j\hat{H}(t_j)\right\}\right\} + O[\delta], \tag{14}$$

which expresses an anti-commutation error $O[\delta]$ between Hamiltonian operators evaluated at different times t_j. The validity of this approximation is discussed in section 4.2.1.
We note from equations (12) and (14) that two numerical errors are respectively involved: (i) a quadrature error resulting from the discretization of the integral and (ii) an anti-commutation error resulting from the decomposition of the exponential operators.

4 Principal Theorems

This section is devoted to theorems 4.1, 4.2, and 4.3.

4.1 Convergence of the rectangular approximation

We present a general result, not restricted to the quantum application.

Definition 4.1. *Given $\{A(t)\}$ as in Definition A.1, define*

$$A_n(t) = A(T[nt/T]/n),\ 0 \leq t \leq T.$$

Here, $[s]$ denotes the greatest integer less than or equal to s. If $s \leq t$, and $s,t \in [t_{j-1},t_j]$, and $A_n \equiv A$ on this interval, then

$$U_n(t,s) = e^{-(t-s)A}.$$

For other values of s, t, $U_n(t,s)$ is uniquely determined by the condition

$$U_n(t,r) = U_n(t,s)U_n(s,r).$$

We make the following observations.

- Convergence of generator approximations as $n \to \infty$:

$$\|A(t) - A_n(t)\|_{Y,X} \to 0, \text{ uniformly}, t \in [0,T].$$

- Invariance and uniform boundedness of evolution operators on Y:

$$U_n(t,s)Y \subset Y, \ \|U_n(t,s)\|_Y \leq C(T), \ \forall t, s, n.$$

- Differentiation:

$$(d/dt)U_n(t,s)g = -A_n(t)U_n(t,s)g, \ g \in Y, \text{ for } t \neq \frac{jT}{n}.$$

Theorem 4.1. *The rectangular rule with $\Delta = T/n$ is globally convergent: for $t, r \in [0,T]$, $r < t$,*

$$\|U(t,r)g - U_n(t,r)g\|_X \leq C\|g\|_Y \ (t-r) \sup_{s\in[0,T]} \|A(s) - A_n(s)\|_{Y,X}.$$

If $t, r \in [t_{j-1}, t_j]$, this global estimate implies the rate of convergence of order $o(\Delta)$. The lengths of the subintervals can be chosen adaptively.

Proof: Consider the identity:

$$U(t,r)g - U_n(t,r)g = -\int_r^t U(t,s)[A(s) - A_n(s)]U_n(s,r)g \, ds, \qquad (15)$$

which follows from the differentiation of $-U(t,s)U_n(s,r)g$ with respect to s, followed by its integration, after the conclusions of Theorem A.1 and the above observations have been introduced. The estimate is now immediate from the uniform convergence of the generator sequence. □

4.2 Optimal or High Precision Quadrature

Although high-precision quadrature is much used (see [31] for a Crank-Nicolson evolution operator approximation), its analysis via approximation theory, including the Bramble-Hilbert lemma and the Sobolev representation theorem, appears minimal. The much older classical theory is described in [32]. To fix the ideas, we consider the method locally, as used on a subinterval originally defined via the rectangular rule. The analysis is not restricted to Gaussian quadrature.

Definition 4.2. *The structure of the Hamiltonian here is assumed of the form written in equation (3), and V has the meaning of a potential. We introduce constants c_j, associated with p interior points t_j of an interval I of length Δ, such that $\sum_{j=1}^{p} c_j f(t_j)\Delta$ is a quadrature approximation for $\int_I f(t)\,dt$. On the interval $[t_0, t_0+\Delta]$, define, for $s \leq t$,*

$$\hat{U}_p(t,s) = \mathcal{T} \exp\left\{ -(t-s) \sum_{j=1}^{p} \frac{i}{\hbar} c_j \hat{H}(t_j) \right\}. \tag{16}$$

We require the constants c_j of the rule to reproduce the spatial part of the operator. There are two parts of the error as seen from approximation theory. There is that determined from the approximate evolution operators, as induced by the quadrature. This is estimated in the following theorem. However, there is also the initial error: that inherited by the quality of the approximation of the solution at the beginning of the local time interval. This is not an input directly controlled.

Theorem 4.2. *Suppose that $\hat{U}$ is invariant on the smooth Sobolev space: $\mathcal{H} = H^{4p}(\Omega) \cap H_0^1(\Omega)$, and $V(x,t)$ is smooth: $V \in C^\infty(\bar{\Omega} \times I)$. Here, I represents the time interval. If the quadrature scheme of Definition 4.2 has precision $2p-1$, then the evolution operators constructed by the approximation scheme satisfy the estimate in $B[\mathcal{H}, L^2]$: for any g of norm one in $\mathcal{H}$,*

$$\|\hat{U}(t_0+\Delta, t_0)g - \hat{U}_p(t_0+\Delta, t_0)g\|_{L^2} \leq C(p,V)\Delta^{2p}.$$

Here, $C(p,V)$ is proportional to a reciprocal Taylor factorial in $2p$; the supremum (over Ω) of the $H^{2p}(I)$ norm of V is the dominant V-contribution.

Proof: We begin with (15), with a re-interpretation of $A(s) - A_n(s)$ as a difference of potentials:

$$A(s) - A_n(s) \mapsto \frac{i}{\hbar}[V(\cdot\,, s) - V_p(\cdot\,)],$$

where V_p is defined by $V_p = \sum_j c_j V(\cdot\,, t_j)$. We emphasize that the sum defining V_p is to be taken as *time ordered*. We have used the reproduction of the spatial part of the operator by the quadrature scheme in writing this reduction. Thus, we have from (15), with $r \mapsto t_0, t \mapsto t_0 + \Delta$:

$$\hat{U}(t_0+\Delta, t_0)g - \hat{U}_p(t_0+\Delta, t_0)g =$$

$$-\frac{i}{\hbar} \int_{t_0}^{t_0+\Delta} \hat{U}(t_0+\Delta, s)[V(\cdot\,, s) - V_p(\cdot\,)]\hat{U}_p(s, t_0)g\, ds. \tag{17}$$

We add and subtract the following quadrature estimator function within the integrand of (17):

$$\mathcal{Q}(\cdot\,) = \sum_{j=1}^{p} \frac{i}{\hbar} c_j \hat{U}(t_0+\Delta, t_j)V(\cdot\,, t_j))\hat{U}_p(t_j, t_0)g.$$

This gives two terms, equivalent to quadrature estimation for two distinct functions:

$$\hat{U}(t_0+\Delta,t_0)g-\hat{U}_p(t_0+\Delta,t_0)g=$$
$$-\frac{i}{\hbar}\int_{t_0}^{t_0+\Delta}[\hat{U}(t_0+\Delta,s)V(\cdot\,,s)\hat{U}_p(s,t_0)g-\mathcal{Q}(\cdot\,)]\,ds$$
$$+\frac{i}{\hbar}\int_{t_0}^{t_0+\Delta}[\hat{U}(t_0+\Delta,s)V_p(\cdot\,)\hat{U}_p(s,t_0)g-\mathcal{Q}(\cdot\,)]\,ds. \tag{18}$$

It remains to estimate the linear functionals summed above in (18), and defined by the difference of integration and quadrature evaluation in each case. Although the hypotheses of the Bramble-Hilbert Lemma [33, Theorem 2] are directly satisfied, the conclusion is not sufficient: this implies an order $O(\Delta^{2p})$ approximation multiplied by a time integrated expression, involving the $2p$-th derivative of V. To obtain a more precise error estimate, also involving the factorial, and required here, we (additionally) apply the Sobolev representation theorem (see [16, Prop. 4.1.1]). This provides the full, triple product estimate, which includes the (Taylor) factorial. Since this estimate is maintained with respect to integration over Ω, the proof is concluded. $\square$.

4.2.1 Evaluation of the quadrature rule approximation

In practice, equation (14) offers an attractive numerical alternative to the original Magnus expansion [8] when applied to large systems. The product of exponentials does not require the manipulation of commutators, and it can also be addressed very efficiently using our FEAST spectral approach (more details will follow in the simulation section). Note that the iteration of the semigroup exponentials in equation (14) represents a slight weighted version extension of the rectangular rule to unequally spaced nodes. One can adapt the proof of Theorem 4.1 to this case to obtain a convergence order of $O(\delta)$. However, it does not seem possible to improve this estimate to $o(\delta)$ as is possible in the case of the rectangular rule. Note that (15) involves the difference between the generator and the approximate generator; in the case of the rectangular rule, this approximation converges uniformly in norm over the t-interval. This does not appear to be the case for the exponential product, where one cannot assert the local convergence of the generator approximation. However, the program carried out in [9], explicitly up to order eight, proposes an interesting improvement: the definition of a 'nearby' discrete problem, so that the so-called commutator-free product exponential rule discussed here can be applied via adjusted weights to improve convergence. It appears to be an open problem as to the actual computational complexity associated with such improved estimates. We note that, in the simulations of the following sections (see Figure 1), one uses very high-order Gauss-Legendre rules. Remarkably, one sees a very close relation between the predictions of Theorem 4.2 and the actual numerical convergence.

4.3 Global in-time solution for admissible Hamiltonians

We show in this section that a solution for the initial-value problem for the nonlinear Schrödinger equation exists for the admissible Hamiltonians we have introduced in section 2.3. In addition to the regularity assumed for V_{ex} previously, we also require here the existence and boundedness of its time derivative. The exchange-correlation potential is not included in this formulation. We retain the meaning of X, Y in this section, previously established in section 2.3.

Definition 4.3. *For $J = [0, T], T$ arbitrary, define $K : C(J; X) \mapsto C(J; X)$ by*

$$K\phi(\cdot\,, t) = U^{\phi}(t, 0)\Psi_0,$$

where U^{ϕ} has been defined in Proposition A.1 of the appendix, and corresponds to the Hartree potential $W * |\phi|^2$.

Remark 4.1. *We will have need of estimates of $\|U^{\phi}(t, s)\|_X$ and $\|U^{\phi}(t, s)\|_Y$. On the L^2 space X, the operators preserve norm. On $Y = H^2 \cap H_0^1$, the operators $U^{\phi}(t, s)$ have norm which is bounded from above by a constant C with dependency, $C(T, \|S\|_{Y,X}, \|S^{-1}\|_{X,Y}, \|\phi\|_{C(J;X)})$ (see [16, Cor. 6.3.6]).*

Lemma 4.1. *The mapping K is a compact and continuous mapping of $Z = C(J; X)$ into itself.*

Proof. We prove the following, which is essential to both parts of the proof.

- The image under K of any ball $\mathcal{B} \subset Z$ is an equicontinuous family: the distance $\|K\phi - K\psi\|_Z < \epsilon$ if $\|\phi - \psi\|_Z < \delta$. Here, δ is independent of ϕ, and ψ, provided ϕ and ψ lie in a fixed ball of Z. This is implied by:

$$\|K\phi - K\psi\|_Z \leq C_{\psi} T \sup_{0 \leq s \leq T} \|A^{\phi}(s) - A^{\psi}(s)\|_{Y,X} \|\Psi_0\|_Y. \tag{19}$$

Here, $C = C_{\psi}$ is the constant of Remark 4.1. We use a variant of (15) to prove (19):

$$U^{\phi}\Psi_0(t) - U^{\psi}\Psi_0(t) = -\int_0^t U^{\phi}(t, s)[A^{\phi}(s) - A^{\psi}(s)]U^{\psi}(s, 0)\Psi_0 \, ds.$$

A direct estimate implies (19). We now show that this yields the asserted equicontinuity. In particular, we must estimate $\sup_{0 \leq s \leq T} \|A^{\phi}(s) - A^{\psi}(s)\|_{Y,X}$, where the operators A^{ϕ}, A^{ψ} are defined in Proposition A.1, via the Hamiltonians defined there. Clearly, the essential term is:

$$\|(W * |\phi|^2)g - (W * |\psi|^2)g\|_X,$$

which is estimated by an adaptation of inequality (38). Specifically, we have:

$$\|(W * |\phi|^2)g - (W * |\psi|^2)g\|_X| \leq \|W\|_X \||\phi|^2 - |\psi|^2\|_{L^1} \|g\|_X, \tag{20}$$

which, after factorization, is finally estimated via $\|\phi - \psi\|_X$, provided ϕ and ψ lie in a fixed ball of Z. We now prove the continuity and compactness.

- The continuity of K on Z.

This follows from the equicontinuity property proven above.

- The compactness of K.

This is more delicate. If $\mathcal{B}$ is bounded in Z, we show that $\mathcal{K} = K\mathcal{B}$ is relatively compact in Z by use of the generalized Ascoli theorem [34, Theorem 6.1, p. 290]. This requires equicontinuity of the family $\mathcal{K}$, shown above. It also requires that

$$\mathcal{K}_t = \{u(t) : u \in \mathcal{K}\}$$

is relatively compact in X for each $t \in J$. Since Y is compactly embedded in X, it is sufficient to show that $\mathcal{K}_t$ is bounded in Y for each $t \in J$. However, an application of Remark 4.1 immediately implies this. This concludes the proof. □

Theorem 4.3. *The mapping K has a fixed point Ψ. In particular, Ψ satisfies the regularity: $\Psi \in C(J;Y) \cap C^1(J;X)$, and the equation:*

$$i\hbar\frac{\partial\Psi(t)}{\partial t} = -\frac{\hbar^2}{2m}\nabla^2\Psi + V_{\text{ex}}\Psi + (W * |\Psi|^2)\Psi,\ \Psi(\cdot\,,0) = \Psi_0.$$

Proof. We use the Leray-Schauder theorem [35]. Suppose $u = sKu$, for some s, where $0 < s \leq 1$. It is necessary to establish a bound for u in Z, which is independent of s; note that u, in general, depends on s. It is easier to work with $\Psi = Ku$, which satisfies the initial value problem:

$$i\hbar\frac{\partial\Psi(t)}{\partial t} = -\frac{\hbar^2}{2m}\nabla^2\Psi + V_{\text{ex}}\Psi + s^2(W * |\Psi|^2)\Psi,\ \Psi(\cdot\,,0) = \Psi_0. \tag{21}$$

The technique we use is conservation of energy, formulated to include the external potential. We establish the following:

- If the energy is defined for $0 < t \leq T$ by,

$$E_s(t) = \int_\Omega \left[\frac{\hbar^2}{4m}|\nabla\Psi|^2 + \left(\frac{s^2}{4}(W * |\Psi|^2) + V_{\text{ex}}\right)|\Psi|^2\right]\, dx_1dx_2dx_3,$$

  then the following identity holds:

$$E_s(t) = E_s(0) + \int_0^t \int_\Omega (\partial V_{\text{ex}}/\partial r)(\mathbf{x}, r)|\Psi|^2\, dx_1dx_2dx_3dr, \tag{22}$$

where

$$E_s(0) = \int_\Omega \left[\frac{\hbar^2}{4m}|\nabla\Psi_0|^2 + \left(\frac{s^2}{4}(W * |\Psi_0|^2) + V_{\text{ex}}\right)|\Psi_0|^2\right]\, dx_1dx_2dx_3.$$

We first observe that (22) is sufficient to imply that the functions $\{\Psi\}$, and hence the functions $\{u\}$, are bounded in Z; indeed, L^2 gradient bounds for Ψ

are obtained from $E_s(t)$. These bounds depend only on Ψ_0, V_{ex}, and the time derivative of V_{ex}. Note that Ψ has X norm equal to that of Ψ_0.
It remains to verify (22); in fact, we establish its derivative:

$$0 = \frac{dE_s}{dt} - \int_\Omega (\partial V_{\text{ex}}/\partial t)(\mathbf{x}, t)|\Psi|^2 \, dx_1 dx_2 dx_3. \tag{23}$$

We use (21): multiply by $\partial\bar{\Psi}/\partial t$, integrate over Ω, and take the real part. This is a standard technique and yields (23). This concludes the proof. □

5 Numerical Simulations and Discussions

In this section, we propose to illustrate the validity of the Theorems 4.1 and 4.2 using a selected pair of realistic numerical experiments (these examples are not restrictive). The first example in 5.2 considers the real-time propagation of the Kohn-Sham wave functions with an external potential $V(\mathbf{x}, t)$ which is linear in the quantum state. The second example in 5.3 presents the TDDFT real-time propagation model within the adiabatic local density approximation (ALDA), where the potential, which includes both the Hartree and exchange-correlation terms, is non-linear in the quantum state but local in time. In the following, we first describe some elements of the numerical modeling strategy that have been used in both examples including the finite-element discretization, the spectral decomposition of the evolution operator, and the FEAST eigenvalue algorithm.

5.1 Numerical modeling

For a system composed of N_e electrons, the ground state electron density $n(\mathbf{r}) = 2\sum_i^{N_e} |\psi_i(\mathbf{r})|^2$ (i.e. 2 for the spin factor) can be obtained from the solution of the DFT Kohn Sham stationary equation [18]:

$$\left[-\frac{\hbar^2}{2m}\nabla^2 + v_{KS}[n](\mathbf{r})\right]\psi_j(\mathbf{r}) = E_j\psi_j(\mathbf{r}), \tag{24}$$

where the Kohn-Sham potential v_{KS} is a functional of the density and it is conventionally separated in the following way:

$$v_{KS}[n](\mathbf{r}) = v_{ext}(\mathbf{r}) + v_{ion}(\mathbf{r}) + v_H[n](\mathbf{r}) + v_{xc}[n](\mathbf{r}), \tag{25}$$

where v_{ext} is the external potential; v_{ion} is the ionic or core potential; v_H is the Hartree potential which accounts for the electrostatic interaction between the electrons and is the solution of a Poisson equation; and v_{xc} is the exchange-correlation potential which accounts for all the non-trivial many-body effects.
In TDDFT, all the N_e initial wave functions $\Psi = \{\psi_1, \psi_2, \ldots, \psi_{N_e}\}$, which are solutions of the Kohn-Sham system (24), are propagated in time using a time-dependent Schrödinger equation:

$$i\hbar\frac{\partial}{\partial t}\psi_j(\mathbf{r}, t) = \left[-\frac{\hbar^2}{2m}\nabla^2 + v_{KS}[n](\mathbf{r}, t)\right]\psi_j(\mathbf{r}, t), \quad \forall j = 1, \ldots, N_e. \tag{26}$$

The electron density of the interacting system can then be obtained at a given time from the time-dependent Kohn-Sham wave functions

$$n(\mathbf{r},t) = 2\sum_{j=1}^{N_e} |\psi_j(\mathbf{r},t)|^2. \tag{27}$$

In our numerical experiments, we consider the ALDA approach where the exchange-correlation potential v_{xc} in (25) depends locally on time and it is a functional of the local density $n(\mathbf{r},t)$ i.e.

$$v_{KS}(n(\mathbf{r},t)) = v_{ext}(\mathbf{r},t) + v_{ion}(\mathbf{r}) + v_H(n(\mathbf{r},t)) + v_{xc}(n(\mathbf{r},t)). \tag{28}$$

From the propagated wave functions, one can obtain any observable physical quantities such as electron density (27) or current [36, 37].
As discussed in this article, we consider the integral form of (26) defined in (6) along with the time-discretization of the evolution operator given in (12). The discretization of the Hamiltonian operator in real-space is performed using the finite element method. For the choice of the elements, we consider respectively prisms for example 1 and tetrahedra for example 2, using either quadratic P2 or cubic P3 polynomial approximation. If $\mathbf{H}$ denotes the resulting $N \times N$ Hamiltonian matrix at a given time t and if N represents the number of finite-element nodes, the spectral decomposition of $\mathbf{H}$ can be written as follows:

$$\mathbf{D}(t) = \mathbf{P}_t^T \mathbf{H}(t) \mathbf{P}_t, \tag{29}$$

where the columns of the matrix $\mathbf{P}_t$ represent the eigenvectors of $\mathbf{H}(t)$ associated with the eigenvalues regrouped within the diagonal matrix $\mathbf{D}(t)$. Since the N_e propagated states are low-energy states, it is reasonable to obtain very accurate spectral approximations, even by using a partial spectral decomposition, where one considers a number M of lowest eigenpairs much smaller than the size N of the system but greater than N_e (i.e. $N_e < M << N$). In all of our numerical experiments, increasing the value of our choice for M has had no influence on the stability of the solutions. The exact error analysis introduced in this spectral decomposition is proposed as future work in section 6.
Since the discretization is performed using non-orthogonal basis functions (e.g. finite element basis functions), the eigenvalue problem that needs to be solved at given time t takes the generalized form:

$$\mathbf{H}(t)\mathbf{p_i}(t) = \mathrm{d_i}(t)\mathbf{S}\mathbf{p_i}(t), \tag{30}$$

where $\mathbf{S}$ is a symmetric positive-definite matrix, and the eigenvectors $\mathbf{p_i}(t)$ are $\mathbf{S}$-orthonormal i.e. $\mathbf{P}_t^T\mathbf{S}\mathbf{P}_t = \mathbf{I}$ with $\mathbf{P}_t = \{\mathbf{p_1}(t), \mathbf{p_2}(t), \ldots, \mathbf{p_M}(t)\}$. By use of the spectral decomposition of the Hamiltonian (29), the exponential in (14) acts only on the eigenvalue matrix $\mathbf{D}(t)$, and one can show that the resulting matrix form of the time propagation equation is given by:

$$\mathbf{\Psi}(t+\Delta_t) = \mathcal{T}\left\{\prod_{j=1}^{p}\left[\mathbf{P}_{t_j}\exp\left(-\frac{i}{\hbar}\xi\omega_j\mathbf{D}(t_j)\right)\mathbf{P}_{t_j}^T\mathbf{S}\right]\right\}\mathbf{\Psi}(t). \tag{31}$$

In real large-scale applications, a direct solution of the evolution operator has often been considered impractical, since it requires solving a hundred to a thousand eigenvalue problems along the time domain (one eigenvalue problem for each time step). However, we rely on the capabilities of the new FEAST eigenvalue algorithm [3] and solver [4], which is ideally suited for addressing such challenging calculations. FEAST is a general purpose algorithm for obtaining selected eigenpairs within a given search interval. It consists of integrating the solutions of very few independent linear systems for the Green's function $\mathbf{G}(Z) = (Z\mathbf{S} - \mathbf{H})^{-1}$ of size N along a complex contour (typically 8 to 16 contour points by use of a Gauss-Legendre quadrature), and one reduced dense eigenvalue problem arising from a Raleigh-Ritz procedure (of size $M_0 \simeq 1.5M$ in the present case). FEAST relies also on a subspace-iteration procedure where convergence is often reached in very few iterations (~ 3) to obtain up to thousands of eigenpairs with machine accuracy. An efficient parallel implementation can be addressed at three different levels ranging from the selection of the search intervals, to solving independently the inner linear systems along with their own parallel treatment. As a result, the algorithm complexity for performing the spectral decomposition (29) is directly dependent on solving a single complex linear system of size N. In comparison with a Crank-Nicolson scheme where small time intervals are needed and the linear systems need to be solved one after another, the spectral approach allows for larger time intervals and a parallel implementation of FEAST requires only one linear system to be solved by interval. It is important to note that even if M becomes very large, linear parallel scalability can still be obtained using multiple contour intervals and an appropriate parallel computing power. Finally, FEAST is also ideally suited for addressing efficiently the time propagation equation in (31), since it can take advantage of the subspace computed at a given time step j as initial guess for the next time step $j + 1$ in order to speed-up the numerical convergence.

5.2 Example 1

We consider the real-time propagation of the Kohn-Sham quantum states for a Carbon nanotube (CNT) device in interaction with an electromagnetic (EM) THz radiation [7]. In this example, the three dimensional time dependent potential (28) does not depend on the electron density and takes the following form:

$$v_{KS}(\mathbf{r}, t) = v_{eps}(\mathbf{r}) + v_{ext}(\mathbf{r}, t),$$

where v_{eps} is a time-independent atomistic empirical pseudopotential which approximates the effect of v_{ion}, v_H and v_{xc} at $t = 0$, and v_{ext} is a time-dependent external potential applied along the longitudinal direction x of the CNT, i.e., $v_{ext} = v_0((2x - L)/L)sin(\omega t)$ with $x \in [0, L]$, which leads to a constant electric field along the direction of x. For performing the 3D simulations, we consider 6 unit cells of a (5,5) CNT with length $L = 1.98$nm, $v_0 = 5$eV, and $\omega = 2\pi f$, with $f = 200$ THz. In our simulations, all the solution wave functions $\mathbf{\Psi}$ (31) will be propagated from $t = 0$ to $t = 8T$, where $T = 1/f = 5 \times 10^{-15}s$ denotes

the period of the EM radiation. Figure 1 provides the time evolution of the energy expectation for the highest occupied molecular orbital (HOMO level) by using both (i) the rectangular rule and small time-step intervals $\Delta = T/p$, and (ii) the high-order integration rule with a long time-step interval $\Delta = T$ and p interior points.

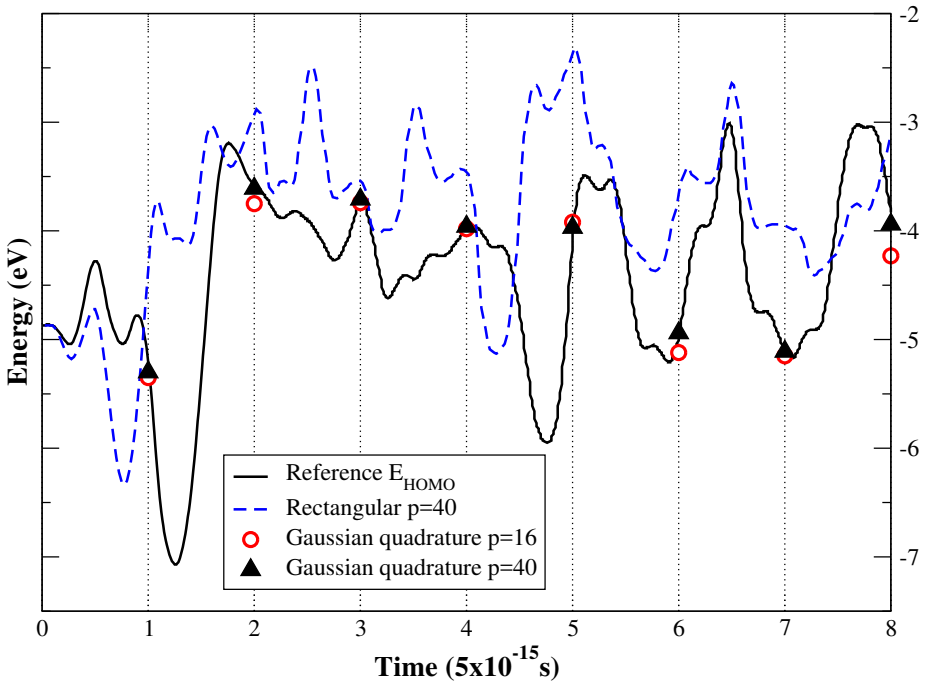

Figure 1: Evolution of the energy expectation of the HOMO level along 8 time periods of the EM THz radiation (i.e. $E(t) = \mathbf{\Psi}^{\dagger}{}_{N_e}(t)\mathbf{H}(t)\mathbf{\Psi}_{N_e}(t)$). The solid lines represent the reference solution. The result for the energy evolution obtained by using a rectangular rule with $p = 40$ diverges after a few time steps. The same number of interior points, however, is adequate to capture the solutions accurately at the end of each time period by using the Gauss quadrature scheme. The solutions obtained using the $p = 16$ Gauss scheme begin to be affected by the approximation constructed from the decomposition of the exponential (14) due to an increase in distance between integration points. We note that the intermediate solutions obtained using the Gauss integration rule have no physical meaning, and are not then represented here.

The reference solutions have been obtained using the rectangular rule and $p = 120$, where the solution has converged. Using a rectangular rule with $p = 40$ integration points by period, one notes that the predicted results begin to diverge after a few time steps, and this phenomenon amplifies with time. From Theorem 4.1, it is necessary to increase p (i.e., decrease the time-step interval) to improve the convergence rate of the rectangular approximation. In contrast, one

can see from the numerical results that $p = 40$ interior points, by using a high-order Gauss integration scheme, does suffice to obtain the solution accurately at each long-time interval Δ. This result can be justified by Theorem 4.2. By decreasing the number of interior points p even further, it is expected to obtain a lower order of approximation. One can indeed confirm a lower convergence rate from the numerical results of the Gauss integration scheme using $p = 16$ interior points. For these lower values of p, one finds convergence comparable to the steps of the exponential product evaluation (14). This emphasizes the higher order convergence of the integration rule (see section 4.2.1).

5.3 Example 2

We now consider the case where the three dimensional time dependent potential (28) depends on the electron density and v_H is the solution of a Poisson equation solved at each time-step. The Poisson equation is solved using the same finite-element mesh as the one used for the Kohn-Sham Hamiltonian, and also using exact boundary conditions at the interfaces of the computational domain (i.e. obtained by solving the integral equation at each node of the interfaces).
This example focuses on obtaining the evolution of the time-dependent dipole moment of the CO molecule by using a real-time propagation approach and the non-linear TDDFT-ALDA model. We follow a similar procedure to that presented in [38] where once the ground-state DFT density and the Kohn-Sham states are obtained, a short polarized impulse is applied along the longitudinal or perpendicular direction of the molecule. If z denotes the perpendicular direction of the molecule, after a short delta impulse along z, the Kohn-Sham states (24) are modified as follows:

$$\psi_j(\mathbf{r}, t = 0^+) = \exp(-\imath I z/\hbar)\psi_j(\mathbf{r}, t = 0), \tag{32}$$

where I is the magnitude of the electric field impulse. Thereafter, equation (31) is solved by using a non-linear potential (28) and no external perturbation (i.e. $v_{ext} = 0$). It is also important to note that our simulations are performed by using an *all-electron* model since the potential v_{ion} is not approximated and includes the core potentials. The density obtained at each time step Δ_t, is used to compute the induced dipole of the system:

$$D(t) = \int_\Omega \mathbf{r}\,(n(\mathbf{r}, t) - n(\mathbf{r}, 0))\,\mathbf{dr}, \tag{33}$$

which is relative to the center of mass of the molecule. $D(t)$ is a quantity of interest since the imaginary part of its Fourier transform provides the dipole strength function and, for this example, the optical absorption spectrum along with the true many-body excited energy levels. Since we are investigating the optical frequency response rather than the THz response presented in the first example, the time intervals are here chosen relatively shorter. Figure 2 presents the time evolution of the dipole $D(t)$ obtained by using both a rectangular rule with a time-step $\Delta_t = 1 \times 10^{-17}$s and a Gauss quadrature scheme using

$p = 1$ and a time interval $\Delta_t = 2 \times 10^{-17}$s. For the Gauss-scheme, a matrix exponential has to be evaluated at the middle of the interval $[t, t + \Delta_t]$ for each t+(1×10^{-17})s (i.e. Gauss-1 presents only one node in the middle of the interval). One notes that both curves are identical at the early stage of the time evolution,

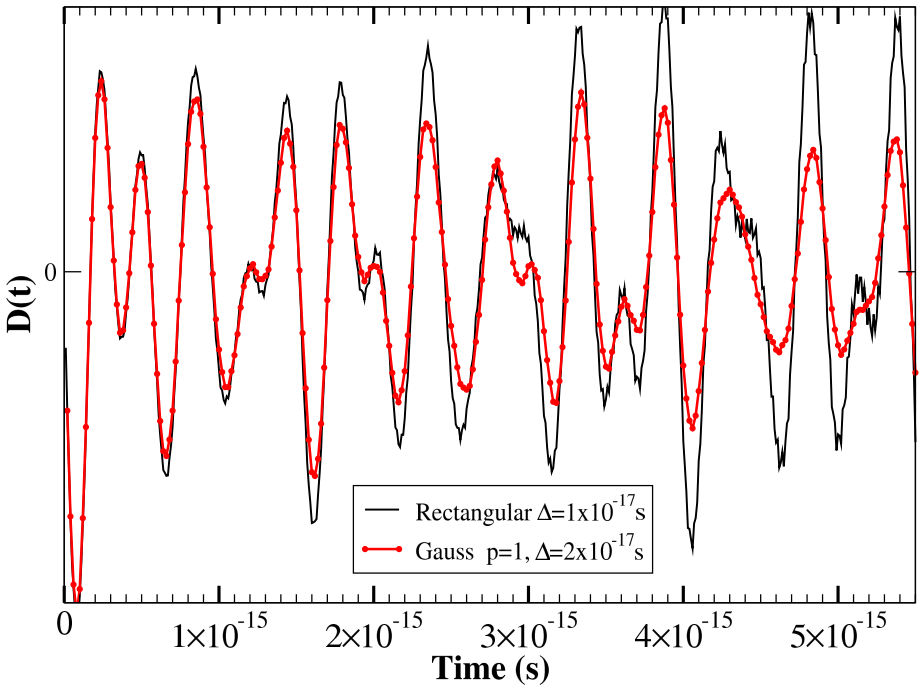

Figure 2: Time evolution of induced dipole moment of the CO molecule after a short-impulse along the perpendicular direction. The results for the rectangular rule (i.e. direct approach) are obtained by using the time step 1×10^{-17} while a time step of 2×10^{-17} is considered for the Gauss quadrature scheme with $p = 1$. This latter scheme presents then only one interior point in the middle of the interval. Although the variation for the two responses presents a similar pattern, the Gauss-1's curve appears much smoother than the curve obtained using the rectangular approximation.

and present also a similar frequency pattern behavior. However, the rectangular approximation clearly presents a staircase pattern which can be attenuated by using a much smaller time-step as shown in Figure 3. This variation pattern is most likely related to the P^0 approximation used by the rectangular approximation between intervals, while the Gauss-1 scheme is associated with a P^1 approximation. It should be noted, however, that the rectangular rule provides a direct propagation scheme where the potential is always known in advance at a given time step Δ_t. In contrast, the Gauss scheme requires an a priori evaluation of the unknown potential at the p Gauss interior points. In practice, it is

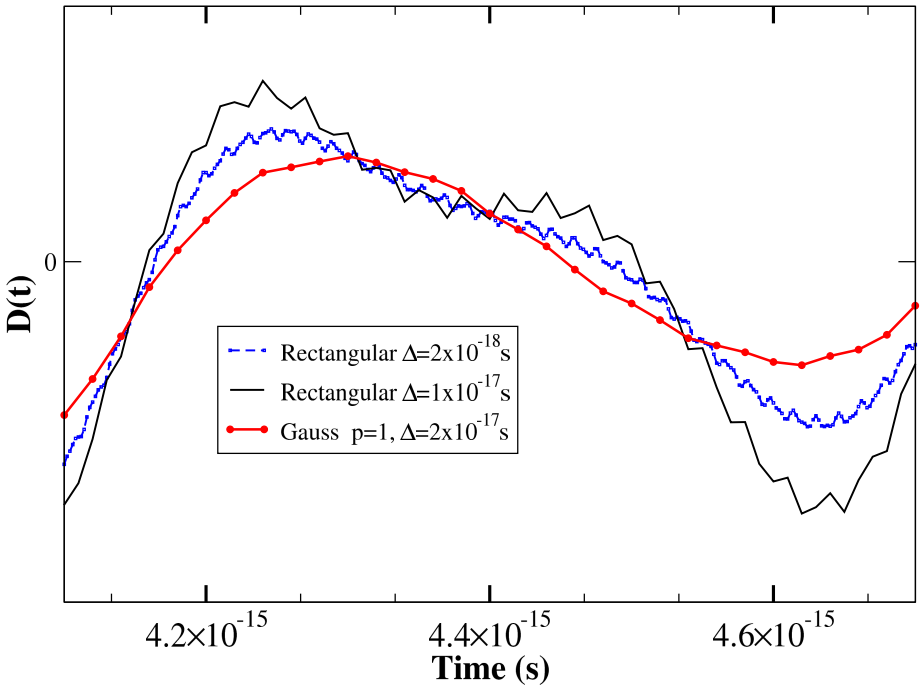

Figure 3: Time-evolution sample of induced dipole moment of the CO molecule after a short-impulse along the perpendicular direction. These results are identical to the one presented in Figure (2) over a selected period in time; the result for a rectangular rule using a much smaller time step, $\Delta_t = 2 \times 10^{-18}$, is also provided for comparison. One notes that the rectangular approximation benefits from shorter time intervals since the resulting curve is both smoother than the one obtained using $\Delta_t = 1 \times 10^{-17}$, and closer to the result obtained using Gauss-1.

possible to use different extrapolation or predictor/corrector schemes, although the overall procedure should ideally be self-consistent [39]. All the models presented in this article where the potential is required to be known beforehand in the time interval, would then remain valid if such a self-consistent iterative procedure occurs. The current example does not take advantage of the self-consistent procedure, and we have then considered only the use of the Gauss-1 propagation scheme where the potential/density is obtained beforehand in the middle of the interval. Interestingly, the Gauss-1 model is known as the exponential mid-point rule by the TDDFT community [23], a robust scheme that also preserves the time-reversal symmetry. Our general analysis offers here some perspectives to go beyond the Gauss-1 scheme in order to provide more accuracy by using longer time-intervals. More details on the absorption spectrum and other physical results obtained by using the Gauss-propagating scheme will be provided elsewhere [40].

6 Future Work and Perspectives

We have presented and analyzed a numerically efficient discretization approach for the general problem of real time propagation of the time-dependent evolution operator. Modern "matrix diagonalization techniques", such as FEAST [3], permit the creation of new methodologies for real-time propagation of large-scale quantum systems using direct integration and discretization of the time-ordered evolution operator. As shown, it is also possible to define an approach that allows a significant reduction of the number of eigenvalue problems which are solved in the time-stepping, due to the smaller number of time step quadratures. Both the number and solution accuracy of these eigenvalue problems contribute to the computational complexity in TDDFT.

- Implicit in the time discretization is the further spectral approximation of the evolution operators, inherent in the eigenvalue/eigenvector calculations. An exact error analysis will incorporate both of these features. In terms of approximation theory, the error introduced by the spectral approximations should be balanced by that of the time discretization.

A detailed analysis of the numerical linear algebra of this spectral approximation step may be found in [7], which appears to be one of the first instances of correlation of this type. If time discretization is measured by the rectangular rule, this permits the flexibility of lower-dimensional intermediate spectral approximation as discussed, and implemented, in [7]. One can note that the techniques proposed here will be extremely efficient for linear physical systems using very large time-intervals. The traditional notions of interacting and non-interacting systems in quantum physics are often used within the context of the single electron picture. Within TDDFT, the many body problem becomes numerically tractable, but also non-linear with respect to the electron density (i.e., interacting system). Since the electron density exhibits much weaker variations as compared to the variations of the individual wave functions, it would

then become advantageous to use time-intervals that are capable of capturing the variation of the electron density with time, while still being much longer than the traditional short-time steps of rectangular approximations. Convergence analysis of a fully non-linear scheme would represent an important step in TDDFT, and it is also a component of our future work. However, local existence is much easier:

- The framework presented here establishes the existence of local in time solutions to certain non-linear TDDFT systems, formulated for closed systems.

This is a consequence of Kato's theory (cf. [41], [16, Th. 7.2.4]), based on the contraction mapping theorem. We simply state, in summary, the character of the result, when the potential is perturbed by a nonlinear function $\phi(\rho)$ of the charge. As long as ϕ is bounded, with bounded derivatives, then the hypothesis of Theorem A.2 holds as long as Y is identified with a Sobolev space of sufficiently high index $s > 5/2$. In this case, the isomorphism from Y to X is implemented by intermediate spaces, described in [42, pp. 244–247]. The other hypotheses of the local existence theorem are routine within the framework developed here. These results are consistent with those obtained by other methods for nonlinear Schrödinger equations [11]. In particular, it includes the case of the exchange-correlation potential. In future work, we will aim for establishing a global in time existence theory, via the evolution operators, for non-linear TDDFT systems, which extends the applicability of Theorem 4.3 and is also consistent with the literature [11].

7 Remarks on equicontinuity in the proof of Lemma 4.1

The arguments there support uniform continuity, thus continuity. We fill in the brief argument for equicontinuity here. This means estimating the L^2 norm of $U^\phi(t_1,0)\Psi_0 - U^\phi(t_2,0)\Psi_0$ in terms of $|t_1 - t_2|$, uniformly for ϕ in a bounded set in L^2. This follows from the representation,

$$\frac{d}{dt}U^\phi(t,0)\Psi_0 = -\hat{H}(t,\rho)U(t,0)\Psi_0,$$

when integrated between t_1 and t_2, and estimated. The estimate is proportional to $|t_1 - t_2|$ since the operator integrand is uniformly bounded over bounded sets.

Acknowledgments

The second author is supported by the National Science Foundation under grants No ECCS 0846457 and No ECCS 1028510.

A Time-Ordered Evolution Operators

Time dependent quantum mechanics is ideally suited to the use of Kato's evolution operators, introduced in [13, 14], improved in [15], and summarized in detail in [16, Ch. 6]. We present a concise summary here, coupled to the hypotheses discussed earlier.

A.1 Defining properties on the frame space X

We briefly summarize the result. We begin with a complex Banach space X and denote by $G(X)$ the family of negative generators of C_0-semigroups on X. We discuss the general case in this section; the case of the Hamiltonian is retrieved by $A(t) \mapsto (i/\hbar)\hat{H}(t)$.

Definition A.1. *If a family $A(t) \in G(X)$ is given on $0 \le t \le T$, the family is stable if there are stability constants M, ω such that*

$$\| \prod_{j=1}^{k} [A(t_j) + \lambda]^{-1} \| \le M(\lambda - \omega)^{-k}, \quad \text{for } \lambda > \omega, \tag{34}$$

for any finite family $\{t_j\}_{j=1}^k$, with $0 \le t_1 \le \cdots \le t_k \le T$. Moreover, $\prod$ is time-ordered: $[A(t_\ell) + \lambda]^{-1}$ is to the left of $[A(t_j) + \lambda]^{-1}$ if $\ell > j$. If Y is densely and continuously embedded in X, and $A \in G(X)$, Y is A-admissible if $\{e^{-tA}\}|_Y$ is invariant, and forms a C_0-semigroup on Y.

These are the preconditions for the theorem on the unique existence of the evolution operators.

A.2 The general theorem for the frame space

The following theorem concatenates [16, Theorem 6.2.5, Proposition 6.2.7].

Theorem A.1. *Let X and Y be Banach spaces such that Y is densely and continuously embedded in X. Let $A(t) \in G(X), 0 \le t \le T$ and assume the following.*

1. *The family $\{A(t)\}$ is stable with stability index (M, ω).*
2. *The space Y is $A(t)$-admissible for each t. The family of generators on Y is assumed stable.*
3. *The space $Y \subset D_{A(t)}$ and the mapping $t \mapsto A(t)$ is continuous from $[0, T]$ to the normed space $B[Y, X]$ of bounded linear operators from Y to X.*

Under these conditions the evolution operators $U(t, s)$ exist uniquely as bounded linear operators on X, $0 \le s \le t \le T$ with the following properties.

I The family $\{U(t, s)\}$ is strongly continuous on X, jointly in (t, s), with:

$$U(s, s) = I, \ \|U(t, s)\|_X \le M \exp[\omega(t - s)].$$

II The time ordering is expressed by:

$$U(t,r) = U(t,s)U(s,r).$$

III If D_t^+ denotes the right derivative in the strong sense, then

$$[D_t^+ U(t,s)g]_{t=s} = -A(s)g,\ g \in Y,\ 0 \le s < T.$$

IV If d/ds denotes the two-sided derivative in the strong sense, then

$$(d/ds)U(t,s)g = U(t,s)A(s)g,\ g \in Y,\ 0 \le s \le t \le T.$$

This is understood as one-sided if $s = t$ or $s = 0$.

An important question in the theory is what condition guarantees that the evolution operators remain invariant on the smooth space Y. This is now addressed.

A.3 A result for the smooth space: regularity

We quote a slightly restricted version of [16, Theorem 6.3.5].

Theorem A.2. *Suppose hypotheses (1,3) of Theorem A.1 hold, and that there is an isomorphism S of Y onto X such that*

$$SA(t)S^{-1} = A(t) + B(t),\ B(t) \in B[X],$$

a.e. on $[0,T]$, where $B(\cdot)$ is strongly measurable, and $\|B(t)\|$ is Lebesgue integrable. Then hypothesis (2) of Theorem A.1 holds. Also, the following hold.

I′ Invariance:

$$U(t,s)Y \subset Y,\ 0 \le s \le t \le T.$$

II′ The operator function $U(t,s)$ is strongly continuous on Y, jointly in s and t.

III′ For each $g \in Y$,

$$(d/dt)U(t,s) = -A(t)U(t,s)g,\ 0 \le s \le t \le T, s < T.$$

This derivative is continuous on X.

A.4 The initial value problem

The evolution operators permit the solution of the linear Cauchy problem,

$$\frac{du}{dt} + A(t)u(t) = F(t), \tag{35}$$

$$u(0) = u_0, \tag{36}$$

on an interval $[0,T]$, with values in a Banach space X. The formal solution,

$$u(t) = U(t,0)u_0 + \int_0^t U(t,s)\ F(s)\ ds, \tag{37}$$

holds rigorously under assumptions on u_0, F (for a precise statement, cf. [16, Prop. 6.4.1]). In particular, the initial-value problem (1,2) is solved by the identifications $u \mapsto \Psi, A \mapsto \frac{i}{\hbar}\hat{H}$, with $F = 0$.

A.5 Admissibility of the Hartree potential

Proposition A.1. *The operators,*

$$\hat{H}^u(t) = -\frac{\hbar^2}{2m}\nabla^2 + V_{\rm ex}(\cdot\,,t) + W * |u(\cdot\,,t)|^2,$$

with domain, $H^2(\Omega) \cap H_0^1(\Omega)$, satisfy the hypotheses of Theorem A.2 for each

$$u \in C([0,T]; L^2(\Omega)).$$

Here, T is an arbitrary terminal time and the identifications,

$$X = L^2(\Omega),\ Y = H^2(\Omega) \cap H_0^1(\Omega),$$

are made. The external potential $V_{\rm ex}$ is assumed continuous from the time interval into the space of twice continuously differentiable functions, with bounded derivatives through order two in $\mathbf{x}$. In particular, the evolution operators $U^u(s,t)$ exist in the sense of Theorem A.2 when the identification $A^u(t) = (i/\hbar)\hat{H}^u(t)$ is made.

Proof. The proof proceeds by verifying hypotheses 1,3 of Theorem A.1 and the similarity hypothesis of Theorem A.2. It is equivalent to use $\hat{H}^u(t)$. We use X, Y for notational convenience in the proof. We note the inequality, for each t,

$$\|(W * |u|^2)g\|_X \leq \|W\|_X \||u|^2\|_{L^1} \|g\|_X, \tag{38}$$

which follows from the Schwarz inequality and Young's inequality. This implies that the Hartree potential defines a bounded linear operator on L^2 for each t. The same is true for $V_{\rm ex}$. This permits the straightforward verification of the Assumption in section 2.2 for the operators $\{\hat{H}^u(t)\}$. In fact, one can employ the Friedrichs extension to the symmetric operator defined on infinitely differentiable compact support functions. The above inequality and the assumed properties of $V_{\rm ex}$ can be used to verify the third hypothesis of Theorem A.1. It remains to verify the similarity relation expressed in Theorem A.2. We define S^{-1} here as the 'solver' for the homogeneous Dirichlet problem for the (negative) Laplacian S on Ω; the boundary is assumed sufficiently smooth to allow for H^2 regularity for the solver when applied to L^2 functions. By direct calculation we have:

$$S\hat{H}^u S^{-1} g = -\frac{\hbar^2}{2m}\nabla^2 g + SV_{\rm ex}S^{-1}g + S(W * |u|^2)S^{-1}g,$$

for $g \in Y$. It is necessary to demonstrate that the second and third operators are bounded on L^2 for each t. For the third operator, one has

$$B(t)g = S(W*|u|^2)S^{-1}g = 4\pi|u|^2 S^{-1}g - 2\sum_{j=1}^{3}(W_{x_j} * |u|^2)(S^{-1}g)_{x_j} + (W*|u|^2)g.$$

Note that we have used the fact that $W/(4\pi)$ defines, by convolution, a right inverse for S. We analyze each of the three terms.

1. For arbitrary t and $g \in X$:

$$\||u|^2 S^{-1} g\|_X \leq \||u|^2\|_{L^1} \|S^{-1} g\|_{L^\infty} \leq C \sup_{0 \leq s \leq T} \|u(\cdot\,, s)\|_X^2 \|g\|_X.$$

   We have used Sobolev's inequality.

2. For arbitrary t, j and $g \in X$:

$$\|(W_{x_j} * |u|^2)(S^{-1} g)_{x_j})\|_X \leq \|(W_{x_j} * |u|^2)\|_{L^{6/5}} \|(S^{-1} g)_{x_j}\|_{L^6} \leq$$

$$C \|W\|_{L^{6/5}} \sup_{0 \leq s \leq T} \|u(\cdot\,, s)\|_X^2 \|g\|_X.$$

   We have used the Hölder, Young, and Sobolev inequalities, as well as the standard computation of partial derivatives of W.

3. For arbitrary t and $g \in X$:

$$\|(W * |u|^2) g\|_X \leq \|(W * |u|^2)\|_X \|g\|_X \leq \|W\|_X \sup_{0 \leq s \leq T} \|u(\cdot\,, s)\|_X^2 \|g\|_X.$$

   We have used Young's inequality and the Schwarz inequality.

This establishes that $B(t)$ is bounded on X for each t. The function space measurability and integrability are discussed in detail in [16, Prop. 7.1.4]. This completes the verification for the final term. The verification for the second term is straightforward. □

References

[1] A. Castro and M.A.L. Marques, Time dependent density functional theory, Lec. Notes in Phys. **706** (2006) 197–210.

[2] T.Y. Mikhailova and V.I. Pupyshev, Symmetric approximations for the evolution operator. Physics Letters A **257**, 1-2 (1999), 1–6.

[3] E. Polizzi, Density-matrix-based algorithm for solving eigenvalue problems. Phys. Rev. B **79** (2009), p115112.

[4] FEAST eigenvalue solver. *http://www.feast-solver.org*

[5] J. Crank and P. Nicolson, A practical method for numerical evaluation of solutions of partial differential equations of the heat-conduction type. Advances in Computational Mathematics **6**, 1 (1996), 207–226.

[6] K. Yajima, Existence of solutions for Schrödinger evolution equations. Comm. Math. Phys. **10** 3 (1987), 415–426.

[7] Z. Chen and E. Polizzi, Spectral-based propagation schemes for time-dependent quantum systems with applications to carbon nanotubes. Physical Review B **82** (2010), 205410 (8 pages).

[8] W. Magnus, On the exponential solutions of differential equations for a linear operator. Commun. Pure Appl. Math. VII (1954), 649–673.

[9] A. Alvermann and H. Fehske, High-order commutator-free exponential time propagation of driven quantum systems. J. Comp. Phys. **230** 15 (2011), 5930–5956.

[10] E. Cancès and C. Le Bris, On the time-dependent Hartree-Fock equations coupled with a classical nonlinear nuclear dynamics. Math. Models Meth. Appl. Sci. **9** 7 (1999), 963–990.

[11] T. Cazenave, *Semilinear Schrödinger Equations*, Courant Institute Lecture Notes 10, 2003, Published by the American Mathematical Society.

[12] A. Elgart, L. Erdös, B. Schlein, and H.-T. Yau, Nonlinear Hartree equation as the mean field limit of weakly coupled Fermions. J. Math. Pures. Appl. (9) **83** 10 (2004), 1241–1273.

[13] T. Kato, Linear equations of hyperbolic type. J. Fac. Sc. Univ. Tokyo **17** (1970), 241–258.

[14] T. Kato, Linear equations of hyperbolic type II. J. Math. Soc. Japan **25** (1973), 648–666.

[15] J.R. Dorroh, A simplified proof of a theorem of Kato on linear evolution equations. J. Math. Soc. Japan **27** (1975), 474–478.

[16] J.W. Jerome, *Approximation of Nonlinear Evolution Equations*, Academic Press, New York, 1983.

[17] W. Kohn and P. Vashista, General density functional theory. *Ch. 2, Theory of the Inhomogeneous Electron Gas* (Plenum Press, New York, 1983).

[18] W. Kohn and L. J. Sham, Self-consistent equations including exchange and correlation effects. Phys. Rev. **140** (1965) A1133 - A1138.

[19] E. Prodan and P. Nordlander, On the Kohn-Sham equations with periodic background potentials. J. Stat. Phys. **111** (2003), 967–992.

[20] A. J. Freeman and E. Wimmer, Density functional theory as a major tool in computational materials science. Annual Reviews of Material Science **25** (1995), 7–36.

[21] E. Runge and E.K.U. Gross, Density functional theory for time dependent systems. Physical Review Letters **52** (1984), 997–1000.

[22] C. Le Bris and P.-L. Lions, From atoms to crystals: a mathematical journey. Bull. Amer. Math. Soc. (N.S.) **42** (2005), no. 3, 291–363.

[23] A. Castro, M.A.L. Marques, and A. Rubio, Propagators for the time-dependent Kohn-Sham equations. J. Chem. Phys. **121** (2004), 3425–3433.

[24] M. Stone, Linear transformations in Hilbert space, IV. Proc. Nat. Acad. Sci. USA **15** (1929), 198–200.

[25] P.D. Lax, *Functional Analysis*, Wiley-Interscience, New York, 2002.

[26] T. Kato, Fundamental properties of Hamiltonian operators of Schrödinger type. Trans. Amer. Math. Soc. **70** (1951), 195–211.

[27] T. Kato, On the existence of solutions of the helium wave equation. Trans. Amer. Math. Soc. **70** (1951), 212–218.

[28] W. Caspers and G. Sweers, Point interactions on bounded domains. Proc. Roy. Soc. Edinburgh Sect. A **124** (1994), no. 5, 917–926.

[29] A.P. Calderón, Commutators of singular integral operators. Proc. Nat. Acad. Sci. **53** (1965), 1092–1099.

[30] T. Sauer, *Numerical Analysis*, Pearson Addison Wesley, 2006.

[31] L. Lehtovaara, V. Havu, and M. Puska, All-electron time-dependent density functional theory with finite elements: Time-propagation approach. J. Chemical Physics **135** (2011), 154104.

[32] J. Stoer and R. Bulirsch, *Introduction to Numerical Analysis*. Third edition. Texts in Applied Mathematics, 12, Springer Verlag, 2002.

[33] J.H. Bramble and S.R. Hilbert, Estimation of linear functionals on Sobolev spaces with applications to Fourier analysis and spline interpolation. SIAM J. Numer. Anal. **7** (1970), 112–124.

[34] J.R. Munkres, *Topology: A First Course*, Prentice-Hall, 1975.

[35] D. Gilbarg and N. Trudinger. Elliptic Partial Differential Equations of Second Order. Reprint of the 1998 edition, Classics in Mathematics, Springer-Verlag, Berlin, 2001.

[36] E. Polizzi, N. Ben Abdallah, O. Vanbésien, D. Lippens Space Lateral Transfer and Negative Differential Conductance Regimes in Quantum Waveguide Junctions. J. Appl. Phys. **87** (2000), 8700-8706.

[37] Z. Chen, E. Polizzi Spectral Modeling and Propagation Schemes for Time-Dependent Quantum Systems. 14th Intern. Workshop on Comput. Elec., IWCE proceedings, pp 295 - 298, 2010.

[38] K. Yabana, T. Nakatsukasa, J.-I. Iwata, and G. F. Bertsch, Real-time, real-space implementation of the linear response time-dependent density-functional theory. Phys. Stat. Sol. (b) **243**, No. 5 (2006), 1121–1138

[39] C. A. Ullrich, Time-Dependent Density-Functional Theory: Concepts and Applications. Oxford University Press, 2012.

[40] T. Addagarla and E. Polizzi, in preparation.

[41] T. Hughes, T. Kato, J. Marsden, Well-posed quasi-linear, second order hyperbolic systems with applications to nonlinear elastodynamics and general relativity. Arch. Rational Mech. Anal. **63** (1977), 273–294.

[42] J.-P. Aubin, *Applied Functional Analysis*, Wiley Interscience, 1979.